Thermal Science and Engineering Progress 51 (2024) 102657

Contents lists available at ScienceDirect

Thermal Science and Engineering Progress

journal homepage: www.sciencedirect.com/journal/thermal-science-and-engineering-progress

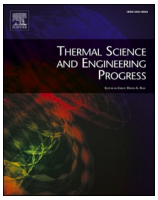

Multi-criteria analysis on the simulation-based optimal design of a new stack-type natural ventilation system for industrial buildings

Onur Kayapinar [a], Aslı E. Arslan [b], Oguz Arslan [a,*], Mustafa Serdar Genc [c,d]

[a] Mechanical Engineering Department, Engineering Faculty, Bilecik Seyh Edebali University, Bilecik, Turkey
[b] Quality Control in Manufacturing Programme, Vocational School, Bilecik Seyh Edebali University, Bilecik, Turkey
[c] Energy Systems Engineering Department, Engineering Faculty, Erciyes University, Kayseri, Turkey
[d] Energy Conversion Research and Application Center, Erciyes University, Kayseri, Turkey

ARTICLE INFO

Keywords:
Exergy analysis
Numerical investigation
Natural ventilation system
Multi-criteria decision-making
Non-direct inputs

ABSTRACT

This study focuses on optimizing a new stack-type natural ventilation system (NVS) designed for industrial buildings. Forty-five different designs were formed in terms of the different NVS sizes. The formed designs were numerically analyzed to determine the performance of the designs. The performance of the designed system was evaluated by exergy analysis. Additionally, the designs were evaluated economically using the net present value (NPV) method. Then multi-criteria decision-making analysis was conducted to determine the optimal solution under the results of economic and exergetic outputs. The input values were selected as non-direct parameters to obtain a homogenous ventilation. As a result, it was determined that implementing this designed model would result in annual savings of 176,922.14 m^3 of natural gas, 331.71 tons of CO_2 emissions, and 0.716 GWh of electricity. The optimum system was determined as investable with an NPV value of 35,475.20 $ for a 20-year lifetime.

1. Introduction

Factory buildings are often characterized by their large volumes, making it challenging to implement ventilation systems. However, for the well-being and comfort of the workers, it is essential to maintain fresh and breathable air inside the building. Considering the increasing energy costs and the impacts of global warming, environmentally friendly and energy-efficient natural ventilation systems (NVS) can offer favorable solutions for the ventilation needs in such buildings. Several natural ventilation systems, such as single-sided, cross, wind towers, solar chimneys, atrium, and stack ventilation, were reported in the literature. These strategies are driven by two main forces: thermal buoyancy and wind-induced forces [1]. Thermal buoyancy-induced ventilation occurs through the pressure difference caused by the temperature difference between indoor and outdoor environments. Wind-induced ventilation occurs through the pressure drop at the ventilation section due to the wind velocity [1,2]. In actual building conditions, the combined effects of these two terms exist [2]. Additionally, the climatic conditions of the location where the building is ventilated are essential parameters determining the NVS's performance. Gao et al. [3] investigated the stack effect of the natural ventilation by shafts. They concluded that NVSs were crucial to consider the performance of smoke exhaust under −low-pressure environments. Boccalatte et al. [4] investigated the effect of NVS on the energy saving of a greenhouse. They indicated that the biggest contribution to energy saving belongs to NVS. Kayapinar and Arslan [5], in their previous study, experimentally investigated the performance of a new stack-type NVS. They concluded the system could operate under winter and summer conditions with a higher exergy efficiency.

From this point, optimal and effective NVS designs are a requirement for adequate and economical ventilation in industrial buildings. Computational fluid dynamics (CFD) is a successful tool considering the expensive and long-running experimental studies. Limited studies in the literature focus on CFD investigation of similar types of buildings. Wang et al. [6] numerically investigated the natural ventilation of titled channels. They indicated that natural ventilation is a successful tool when the slope is greater than 3%. Vaseghi et al. [7] conducted a numerical investigation to observe the passive ventilation of a concept museum building. They concluded that it is possible to reduce the indoor temperature by 4 °C in the summer. According to the study, natural ventilation is an effective tool for the thermal comfort of shared spaces. Ai et al. [8] studied single-sided natural ventilation systems driven by wind in buildings, focusing on isolated buildings. However, it was found

* Corresponding author.
E-mail address: oguz.arslan@bilecik.edu.tr (O. Arslan).

https://doi.org/10.1016/j.tsep.2024.102657
Received 25 February 2024; Received in revised form 17 April 2024; Accepted 21 May 2024
Available online 22 May 2024

Nomenclature

A	Area (m^2)
E	Energy, exergy (kW)
C	Cost ($)
P	Pressure (Pa)
T	Temperature (^oC)
V	Volume (m^3)
Q	Flow (m^3/s)
A	Area (m^2)
f	Unit price ($)
R	Universal gas constant (kJ/kmolK)
R^2	Coefficient of determination
SI	Sustainability index
N	Number of NVS unit
HV	Heating value of natural gas(kJ/h)

Greek Letter

ρ	density (kg/m^3)
n	Number of units
*	Average value, perkmole −fuel
φ	Humidity of air (%)
ε	Efficiency (%)
v	Speed (m/s)
ω	Specific Humidity Ratio

Subscript

a	Air
atm	Atmosphere
$building$	Building
c	Operative temperature in FloEFD
da	Dry air
cf	Cash flow
e	Electricity
ec	Electric consumption
exp	Experiment
fan	Required fan instead of NVS
in	Inside
inv	Investment
out	Outside
u	Fluid velocity
L	Labor or Loss
m	Moisture, measurement, mass,
$mean$	Average
ng	Natural gas
r	Speed of wind or discount rate
p	Piping
ph	Physical
s	Saturated
st	Sheet metal
sys	System
t	Welding gas supply temperature
te	Natural gas turbine engine
w	Welding
ws	Welding supply
x	Exergy
wo	Worker or labor

Abbreviations

CFD	Computational Fluid Dynamics
CoV	Covariance
LES	Large Eddy Simulation
LMA	Local Mean Age
NPV	Net present value
NVS	Natural ventilation system
NG	Natural gas
MRT	Mean Radiant Temperature
R^2	Coefficient of determination
$RANS$	Reynolds Averaged Navier–Stokes Equations
$PRMSE$	Proportional Reduction of Mean Squared Error

that the wind flow pattern around a building in an urban environment differs significantly from that around an isolated building due to surrounding buildings. Considering an urban context, this study examines the wind-induced single-sided natural ventilation in nearby buildings along a long street. The change in wind-induced ventilation was determined using the CFD method for the aspect ratios (AR) of 1.0, 2.0, 4.0, and 6.0. As a result, it was found that an increase in the AR ratio leads to a decrease in the ventilation airflow rate. Ali et al. [9] conducted numerical investigations on the impact of angular variation in atrium walls on natural ventilation systems in atrium buildings. They created designs by altering the angular shapes of the atrium walls and performed CFD analysis to analyze these designs and compare the results. It was found that in atrium buildings with high walls, the angular variation of the walls enhances the bouncy effect in the upper parts of the building, improving thermal comfort. However, no significant changes were observed at the ground level. The study concluded that, in atrium buildings, using vertical walls instead of inclined walls is more suitable for natural ventilation. Xu et al. [10] conducted a study to evaluate the performance of natural ventilation and explore its potential for sustainability in a building with complex geometry. They performed CFD analysis to simulate the airflow inside the building. The study concluded that optimizing the natural ventilation system design can reduce the building's energy consumption and improve indoor thermal comfort. Furthermore, the study demonstrated that natural ventilation can be effectively implemented in a building with complex geometry. In their study, Guo et al. [11] optimized natural ventilation systems for green building design using the CFD analysis method. A three-dimensional layout, building shapes, wind speed, and direction were considered for the selected street and building designs, and an optimization method was developed in conjunction with CFD. The study examined the interactions between variables such as ventilation opening size and direction, wind speed, and building shape to investigate their effects on each other. Gianpiero et al. [12] examined the CFD analyses conducted to investigate how wind-driven natural ventilation occurs in buildings and to evaluate its performance. The foundation of the study relies on computer-based Computational Fluid Dynamics (CFD) analyses. A CFD design incorporating the building geometry was created to analyze various scenarios generated by variable wind loads. The study results demonstrate that wind-driven natural ventilation can effectively occur in buildings. Additionally, it was concluded that the CFD analysis method could be used as an alternative to costly experimental tests. Hulsure and Maurya [13] conducted a CFD analysis on a wind-driven natural ventilation system for an industrial storage building in the Embassy Industrial Park Bilaspur, Gurugram, India. Considering different wind loads and environmental conditions, the behavior of the natural ventilation system was determined using the CFD analysis method. As a result, it was concluded that implementing a physical design on the roof ridge and adding extra air intake points on the building's side walls were necessary for optimizing the system. Hooff et al. [14] identified the possible and impossible limitations for conducting CFD analysis on Amsterdam Arena stadium, which included natural ventilation, thermal changes, humidity, and CO_2 concentration. Throughout the study,

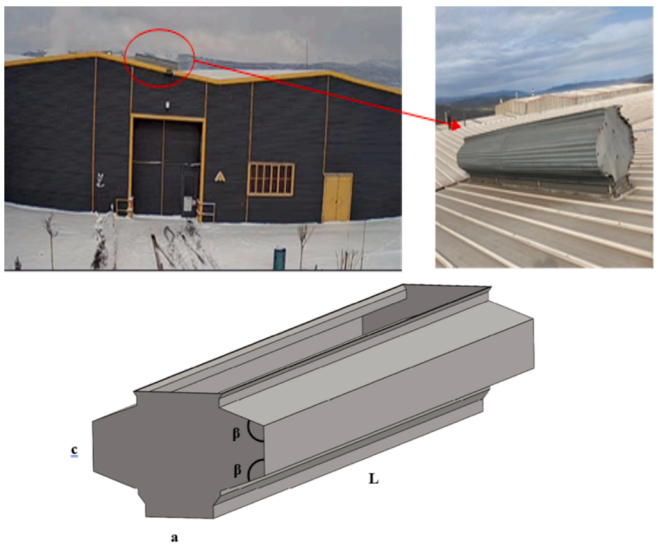

Fig. 1. The schematic and view of the application building and designed NVS.

variations in environmental conditions, the number of people inside the stadium, humidity, and CO_2 concentration were closely measured over three days, with data collected directly from the stadium. The analysis of the scaled stadium design and the experimentally obtained data under real conditions were used to validate the study. For the CFD analysis, the wind blowing around the stadium was assumed to be isothermal and included in the study. Huang et al. [15] conducted a numerical analysis that included wind effects on the Commonwealth Advisory Aeronautical Council steel building. They employed Computational Fluid Dynamics (CFD) techniques, such as Large Eddy Simulation (LES), Reynolds Averaged Navier–Stokes Equations (RANS) Design, and others, to predict wind loads on and wind flows around the building. The primary objective of their study was to investigate an effective and reliable approach for evaluating wind effects on tall buildings using CFD techniques. Rafaela et al. [16] aimed to review experimental and numerical methodologies for investigating high airflow rate natural ventilation systems. A scientific framework, including experimental and numerical analyses, supported the study. The study's results indicated that temperature, air velocity, and relative humidity values were crucial in validating experimental and numerical methods for high airflow rate natural ventilation systems. Twam et al. [17] studied the wind-driven natural ventilation mechanism in venturi-shaped roofs, considering different design designs, using wind tunnel experiments and CFD analysis. Different designs were created at a scale of 1:100 and subjected to wind tunnel experiments. RANS and RNG k-ε designs were used for the CFD analysis. The study revealed that venturi-shaped roofs without louvers provided greater wind-driven ventilation than those with louvers. Additionally, louvers in the designs resulted in pressure losses against the wind, which reduced the ventilation force generated by the wind. These findings were obtained through the analysis of data obtained from the wind tunnel experiments and the results of the CFD analysis.

Although CFD enables the analysis of the systems with less effort and cost, it is still hard to make a decision on the most efficient design. Especially for system designs such as NVSs, including non-parametric decision points such as homogeneous ventilation of buildings, the multi-criteria decision-making (MCDM) analysis would be useful to determine the best design [18–20]. In the literature limited studies were conducted on the MCDM analysis of NVSs. Yin et al. [21] investigated the natural ventilation through windows to measure the ventilating performance. They investigated the non-parametric points such as opening percentage, furniture locations, and window types. First, they analyzed the parameter effects by analysis of variance, and optimized the decision units by gray relational analysis. Wen et al. [22] conducted an optimization of underground natural ventilation through the form and environmental characteristics. They simulated the passive ventilation strategies with CFD and building energy simulators. Then, they optimized the parameters of cooling and heating temperatures, mechanical and natural ventilation rates, internal window operation, and roof construction by a two-level method including uncertainty-sensitivity analysis and Pareto front method based on the genetic algorithm. Liu et al. [23] conducted an optimizing model for the performance of membrane energy exchangers in residential ventilation through influential factors. They used Pareto solutions based on a genetic algorithm for the factors of moisture recovery effectiveness, total membrane area, and operating airflows. Buonomano et al. [24] investigated a new model to enhance the air quality of buildings through novel criteria in light of current ventilation standards addressing the current pandemic scenario. This new model combines the building energy simulation and contagion risk assessment through the Wells-Riley model. Zhang et al. [25] optimized the operation of the stratum ventilation for the heating mode. They used a CFD model verified by experimental data to simulate operational parameters such as thermal comfort, air quality, and energy efficiency. They used a technique of order preference by similarity to the ideal solution (TOPSIS) to obtain the optimal solution. Bianco et al. [26] investigated the effect of phase change material used in the heat recovery and ventilation system. They used the Pareto approach based on the genetic algorithm to optimize the proposed system in terms of indoor air quality and energy consumption.

A new NVS with a structure patented by the Turkish Patent and Trade Mark Office with the registration no of 2019/08313 was experimentally performed in the previous study of authors for an industrial building to remove the non-breathable gases [5,27]. Since the system is successful for both the summer and winter conditions, the optimization of the new design was conducted in this study. The formed designs appropriate to industrial buildings were performed via CFD. The designed NVSs were evaluated through exergy analysis to measure the performance and the net present value (NPV) analysis to measure the economics. Finally, the observed designs were optimized by the multi-criteria decision-making (MCDM) method namely the efficiency analysis technique with output satisficing (EATWOS). In the optimization, economic outputs (NPV), exergetic results, and sustainability index (SI) were used as the output parameters. Contrary to the conventional studies, the non-direct parameters were selected as the input parameters to obtain homogenous ventilation. In this aim, the inverse of the required number of NVS and the covered area were used as the inputs. The environmental evaluation was also performed for the best design under regional conditions.

2. Material and method

2.1. Study area

The study area is a small-scale industrial building with frequently used welding manufacturing methods. The building is located in Bozuyuk industrial zone. The building has a volume ($V_{building}$) of 130,165.0 m^3 with a width of 75 m, a length of 204 m, and a height of 8.5 m. Due to the non-breathable welding gases, removing them from the building is an obligation for better employee comfort. So, a new concept NVS design was conducted and installed, as given in Fig. 1 [5,28]. The building has no extra heating, mechanical ventilation, or air conditioning unit. The ventilation needs in both the summer and winter periods are just served by the new concept design NVS system. The new NVS was placed on the roof of the building to provide ventilation through the stack effect since it was designed to remove waste gases during production. The NVS has a structure consisting of sheet metal to withstand high wind loads and external physical effects such as strong precipitation.

The 45 designs were formed by dimensional scaling the existing

Table 1
The properties of generated designs.

Design no	a (mm)	c (mm)	β(°)	Design no	a (mm)	c (mm)	β(°)
1	1200	250	90	**24**	500	450	110
2	1200	350	90	**25**	500	250	120
3	1200	450	90	**26**	500	350	120
4	1200	250	100	**27**	500	450	120
5	1200	350	100	**28**	500	250	130
6	1200	450	100	**29**	500	350	130
7	1200	250	110	**30**	500	450	130
8	1200	350	110	**31**	300	250	90
9	1200	450	110	**32**	300	350	90
10	1200	250	120	**33**	300	450	90
11	1200	350	120	**34**	300	250	100
12	1200	450	120	**35**	300	350	100
13	1200	250	130	**36**	300	450	100
14	1200	350	130	**37**	300	250	110
15	1200	450	130	**38**	300	350	110
16	500	250	90	**39**	300	450	110
17	500	350	90	**40**	300	250	120
18	500	450	90	**41**	300	350	120
19	500	250	100	**42**	300	450	120
20	500	350	100	**43**	300	250	130
21	500	450	100	**44**	300	350	130
22	500	250	110	**45**	300	450	130
23*	500	350	110				

*Existing design (experimentally investigated for validation) [5].

(experimental) design, resulting in changes in geometric sizes. In this regard, the width (a) was arranged in different sizes to measure the cross-sectional flow area. Besides, the height (c) and β angle were arranged in different sizes to measure inner flow characteristics. The length (L) was kept constant at 6000 mm. Table 1 specifies the dimensional characteristics of designs.

2.2. Numerical analysis

The numerical analysis was employed to determine the performance of the new concept design NVS using SIEMENS FloEFD software. The FloEFD software is used to model the flow and heat transfer mechanisms of the new concept design NVS. The Navier-Stokes, energy, and continuity equations, which are formulations of the laws of conservation of mass, momentum, and energy for fluid flows and heat transfer problems, are solved using FloEFD CFD software. Moreover, laminar and turbulent flows may be predicted using turbulence models in FloEFD. The reason for choosing FloEFD CFD software in this study is that this CFD software is both more practical and faster in industrial applications compared to other widely used CFD software [29–31]. For modeling a new concept NVS system patented on an industrial application, this software has facilitated modeling in the industry. In addition, this CFD software is also very successful in the numerical modeling of complex problems [29–31].

The Reynolds-averaged Navier-Stokes approach (RANS) was solved using a pressure and density-based formulation in FloEFD. The modified k-ε model was selected as the turbulence model. With this model, both turbulence effects and viscous effects [32] that will occur at low speeds, as in this study, can be successfully modeled.

2.3. Grid independency study

The sensitivity of the physical problem solution increases with finer mesh. However, lengthier processing times will result from finer resolutions, thus it's important to understand how fine a resolution is required. With faces aligned with the Cartesian coordinate system, the mesh cells in FLOEFD are rectangular parallelepipeds. The coordinate system's axes and the geometry's flat surfaces line up. The cells close to the boundary are divided by straight lines due to the geometry's original curvature. There is a single-cell center for the split cells on both sides of the border.

The velocity profile increases exponentially with proximity to the wall, whereas the velocity at the wall is zero. The researchers use a few thin cells near the wall to obtain these gradients; however, since wall functions are used in FloEFD, this is not necessary. Rather than

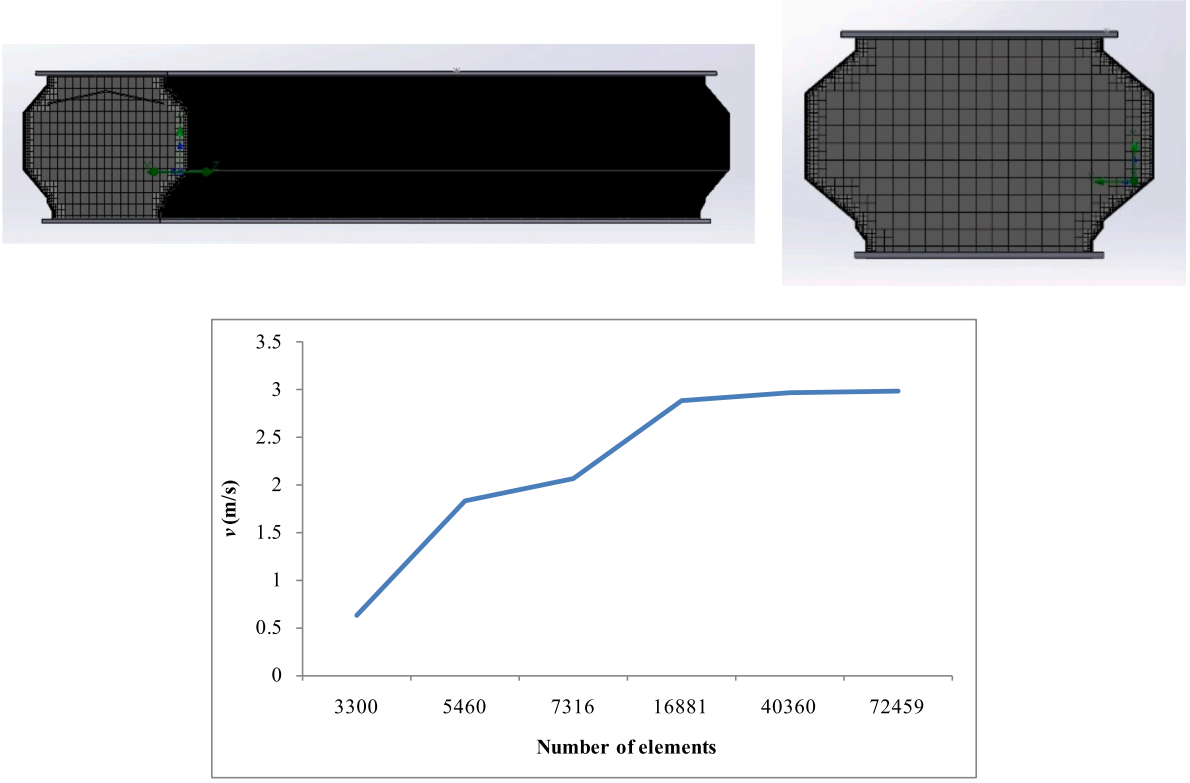

Fig. 2. Schematic of the mesh structure and mesh sensitivity.

Table 2
Analysis conditions for validation.

Analysis no (n)	$T_{outdoor}$(°C)	T_{indoor}(°C)	v_r(m/s)	φ(%)
1	23.2	28.9	3.3	21.1
2	22.8	28.9	2.8	26.5
3	20.0	28.1	3.0	45.8
4	16.7	26.9	3.0	61.2
5	15.6	26.4	2.5	62.7
6	14.7	26.0	2.3	64.8
7	13.2	25.6	2.6	67.6

computing the flow in this area, wall functions model the flow near the wall using experimental data. The number of cells utilized to cover the boundary layer determines the wall functions to be employed in FLOEFD. The flow in this study was computed using the turbulent Van Driest wall function hypothesis.

The mesh generation of the flow domain of the NVS was performed in FloEFD commercial software (see Fig. 2). The mesh structure was refined in terms of the boundary layer. The effect of mesh number (mesh independence) was evaluated on the analysis results. Since the variation in the velocity is negligible after the 16,881 elements, the mesh size and structure with 16,881 elements in Fig. 2 was used in the numerical analysis.

2.4. Model validation

The results of the CFD model were validated with the experimental results of the existing system (Design 23) [5]. The existing implemented design was scaled to 1:1 for the CFD analysis under the conditions specified in Table 2. Different outdoor temperatures ($T_{outdoor}$), indoor temperatures (T_{indoor}), wind speeds (v_r), and relative humidities (φ) were selected in this way. In the selection of these parameters, the worst conditions and the incidence rates were handled. So, the conditions nearest the worst ones with the higher frequency were considered in the analysis.

For the validation, the provided airflow rates ($Q_{T,exp}$) obtained from the experimental study [5,28] regarding the specified conditions were compared with the airflow rate ($Q_{T,CFD}$) calculated by the CFD:

$$Q_{T,\ CFD} = A.v_{\mathrm{CFD}} \tag{6}$$

where A is the cross-sectional area of the NVS system, and v_{CFD} is the average velocity obtained by CFD. The validation results of experiments ($Q_{T,exp}$) and CFD analysis ($Q_{T,CFD}$) are given in Fig. 3.

The results were statistically evaluated using the percentage root mean square error (*PRMSE*), coefficient of variance (*CoV*), and coefficient of determination (R^2) as follows [33]:

$$R^2 = 1 - \frac{\sum y_{output}}{\sum y_{actual}} \tag{7}$$

$$PRMSE = \sqrt{\frac{\sum \left(\frac{y_{output} - y_{actual}}{y_{output}}\right)^2}{n_a}} \bullet 100 \tag{8}$$

$$CoV = \left(\frac{\sum \frac{y_{output} - \widehat{y}_{output}}{y_{actual} - \widehat{y}_{actual}}}{n_a}\right) \bullet 100 \tag{9}$$

where y_{output}, y_{actual}, $\widehat{y}_{output}$ and $\widehat{y}_{actual}$ are CFD output, experimental output, the mean value of the CFD outputs, and the mean value of the experimental outputs, respectively. The obtained results of the statistical evaluation are given in Table 3.

According to the statistical evaluation, *PRMSE*, *CoV*, and R^2 values were obtained as 4.14 %, 8.42 %, and 0.95, respectively. The minimum and maximum errors were recorded as 0.62 % and 5.57 %, respectively. So, the validation indicates an acceptable level of agreement.

2.5. Energy and exergy analysis

The energy and exergy analysis is based on the numerical results of this study. The balance equations were established for the control volumes under steady-state conditions. In this aim, the design for the ventilation of the space is conducted as given in Fig. 4.

The forty-five different designs have the same operating principle, and the data on factors such as the number of employees in the building where the experimental study was conducted, and the quantity of the source gases were obtained from the experimental study [5,28]. Continuous flow conditions apply to the created ventilation designs, and the energy and exergy equations are provided below. The mass balance

Table 3
Statistical evaluation of modeling.

	Statistical parameter				
	PRMSE(%)	*CoV*(%)	R^2	Error (%) Max.	Min.
Value	4.14	8.42	0.95	5.57	0.62

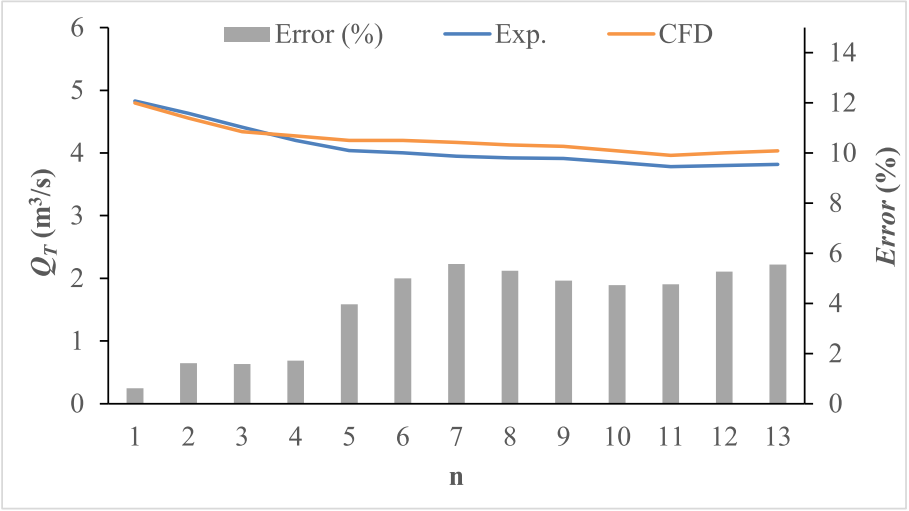

Fig. 3. Model validation.

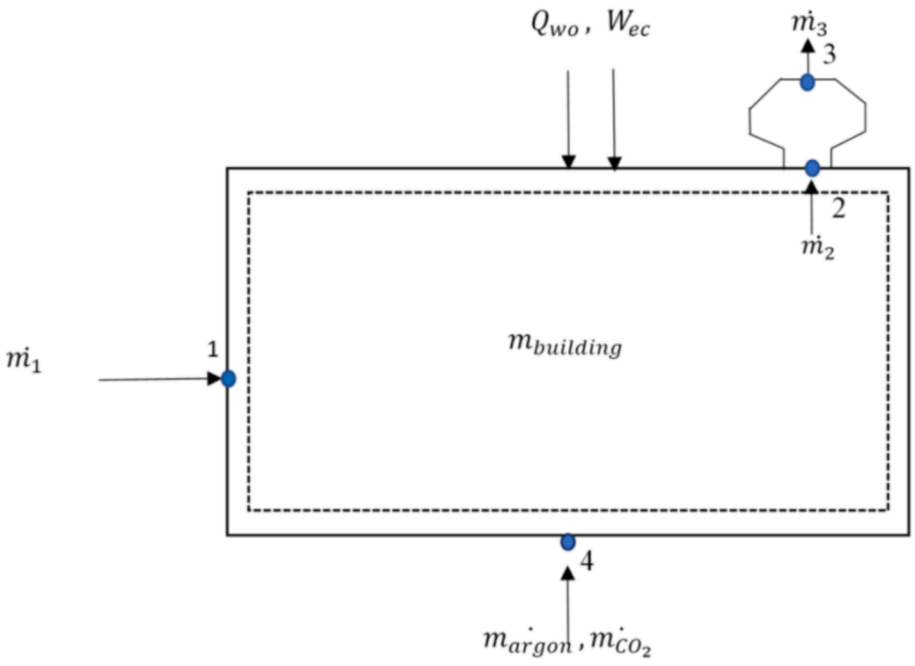

Fig. 4. Design of the natural ventilation system.

Table 4
The emissions of the NG combustion [40,41].

Fuel	Emission (mole)			
	CO_2	CO	NO_x	SO_2
NG*	1.0074	0.0003	0.0254	–

*per mole-fuel.

Table 5
Boundary conditions for CFD analysis.

Parameter	Summer	Winter
T_{in} (°C)	20	20
$T_{enviroment}$ (°C)	13.24	3.42
v_r (m/s)	3.63	4.35
φ (%)	50	50

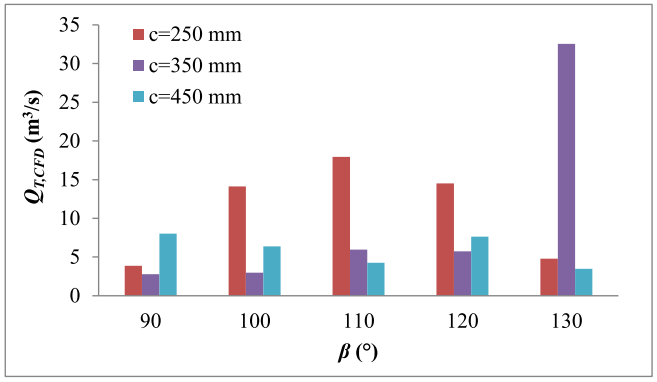

Fig. 5. The effect of β angle and c dimension for $a = 1200$ mm on the flow rate under summer conditions.

equation is constructed considering replacing the ventilated volume (point 2) with the fresh air from the outdoors (point 1). According to this, the mass balance is given by [28]:

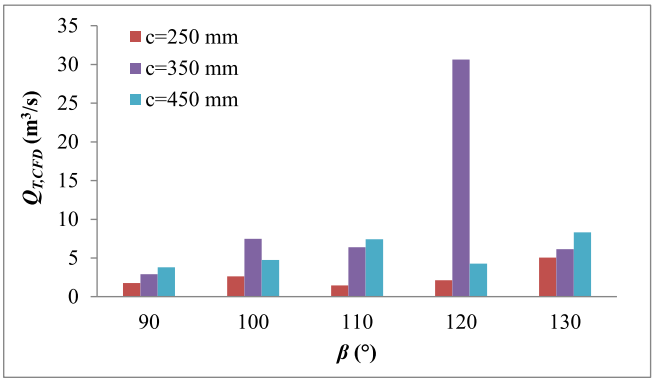

Fig. 6. The effect of β angle and c dimension for $a = 1200$ mm on the flow rate under winter conditions.

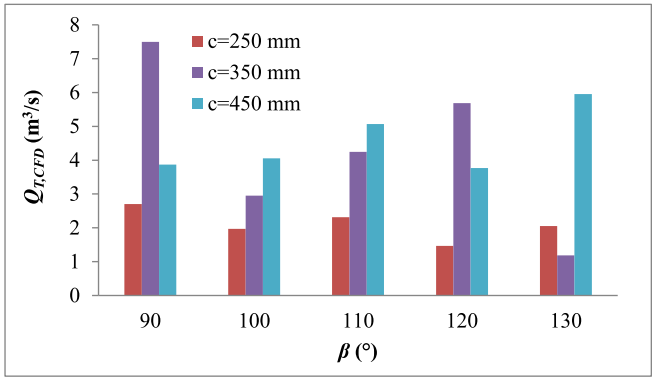

Fig. 7. The effect of β angle and c dimension for $a = 500$ mm on the flow rate under summer conditions.

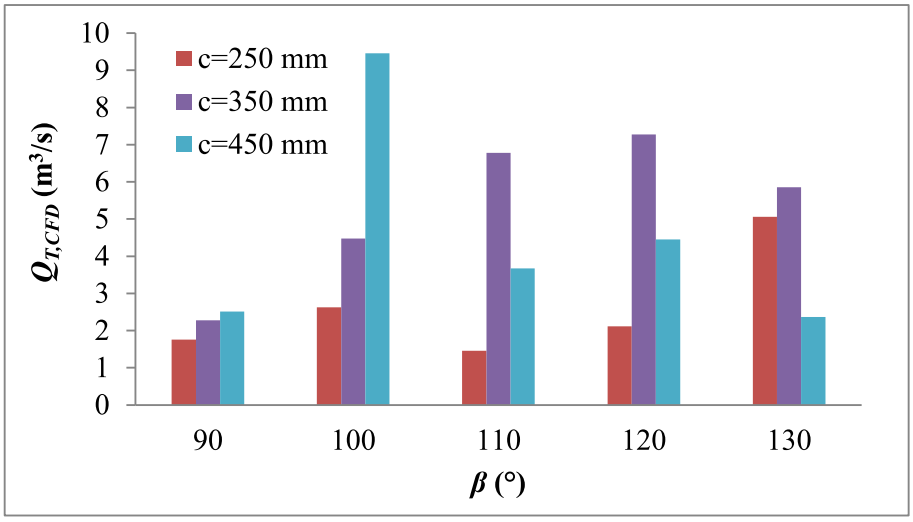

Fig. 8. The effect of β angle and c dimension for a = 500 mm on the flow rate under winter conditions.

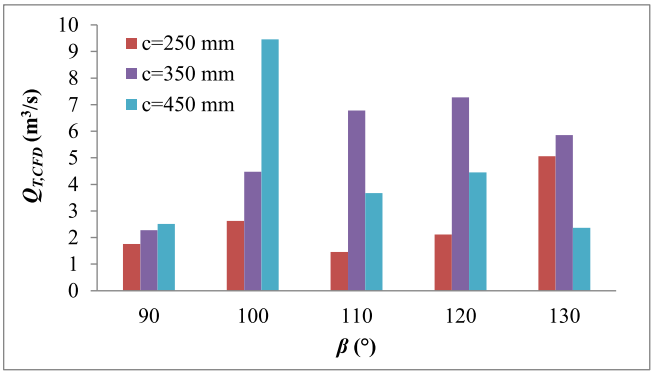

Fig. 9. The effect of β angle and c dimension for a = 300 mm on the flow rate under summer conditions.

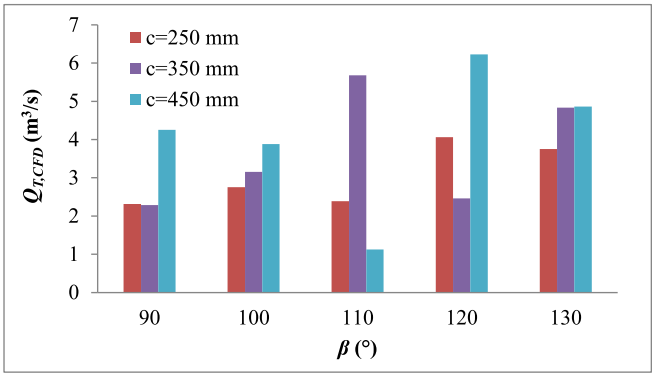

Fig. 10. The effect of β angle and c dimension for a = 300 mm on the flow rate under winter conditions.

$$\overbrace{\rho_{a,1}.\dot{Q}_T}^{\dot{m}_1} + \dot{m}_4 - \overbrace{\rho_{a,2}.\dot{Q}_T}^{\dot{m}_2} = 0 \tag{10}$$

Here $\dot{m}_1$ is the mass rate of air at point 1 (kg/s), $\dot{m}_2$ is the mass rate of air at point 2 (kg/s), and $\dot{Q}_T$ is the volumetric flow rate in NVS (m^3/s). $\dot{m}_4$ indicates the sum of the mass rates of welding gases. The welding gasses used in the production process are argon ($\dot{m}_{argin}$) and CO_2 ($\dot{m}_{CO_2}$). Welding gas consumptions were added to the calculations considering the annual data of Ref [5,28]. Also, the working activity in the building (between 08:30 am and 17:30, six days a week) was considered in the study. In this regard, m_4 was introduced as zero (0) to calculations when there is no operational activity in the building. The density of the building air was assumed to be equal to the density of point 2 ($\rho_{a,building} = \rho_{a,2}$). So, the energy balance is given by [28]:

$$\dot{Q}_{loss} = \left(\dot{m}_2 h_2\right) - \left(\dot{m}_1 h_1\right) - \left(\dot{m}_{argon} h_{argon}\right) - \left(\dot{m}_{CO_2} h_{CO_2}\right) - \left(\dot{W}_{ec}\right) - \left(\dot{Q}_{wo}\right) \tag{11}$$

where $\dot{W}_{ec}$, $\dot{Q}_{loss}$ and $\dot{Q}_{wo}$ are the electricity consumption, heat losses from the building, and the heat loads occurred by the workers, respectively. The enthalpy values of h_1, h_2, h_{argon}, and ^{hCO2} are taken from Ref. [34]. The electricity consumption and heat loads were taken from average data by the industrial company in question [28]. $\dot{m}_{CO_2}$, $\dot{m}_{argon}$, and $\dot{m}_{air}$ are the mass rate of CO_2, argon, and moist air, respectively. h_{CO_2}, $h_{argon,}$, h_{air} are the enthalpy of CO_2, argon, and moist air, respectively. For the active working period, these values are calculated by [5,28]:

$$h_{air} = 0.142 \bullet 10^{-7} \bullet T^3 + 0.855 \bullet 10^{-4} \bullet T^2 + + 0.993 \bullet T + 273.31 \tag{12}$$

$$h_{CO_2} = 7.94 \bullet T_t^4 - 33.69 \bullet 10^{-6} \bullet T_t^3 + 55.18 \bullet 10^{-3} \bullet T_t^2 + 24.99 \bullet T_t - \left(\frac{0.136 \bullet 10^6}{T_t}\right) \tag{13}$$

$$h_{argon} = 1.09 \bullet 10^{-8} \bullet T_t^4 - 1.46 \bullet 10^{-7} \bullet T_t^3 + 2.87 \bullet 10^{-7} \bullet T_t^2 + 20.78 \bullet T_t - \left(\frac{3.661 \bullet 10^{-8}}{T_t}\right) \tag{14}$$

where ω_{air} specific humidity ratio of air (kg/kg-dry air), T is the temperature of air (°C), and T_t is the welding gas supply temperature, equal to indoor temperature. Finally, the exergy balance of the system is given by:

$$\dot{E}x_{in} - \dot{E}x_{out} - \dot{E}x_d - \dot{E}x_Q + \dot{E}x_W + \dot{E}x_{wo} = 0 \tag{15}$$

where $\dot{E}x_{in}$ and $\dot{E}x_{out}$ are the inlet and outlet exergy of the flows, respectively. Ex_d is the destructed exergy,Ex_Q is the exergy due to the

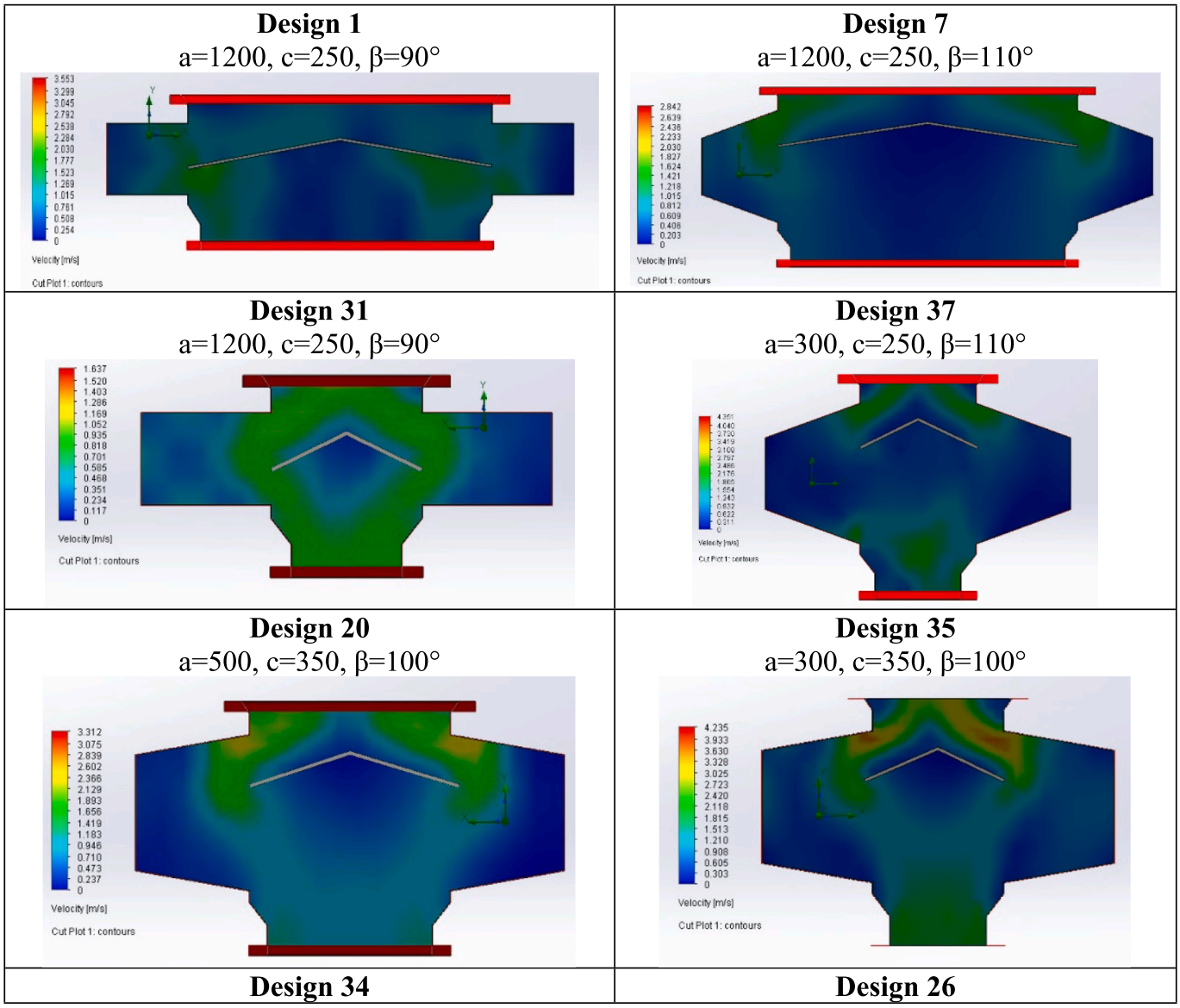

Fig. 11. Velocity distributions for different designs under summer conditions.

heat loads, Ex_W is the work (electricity) exergy, and Ex_{wo} is the labor exergy. The chemical exergies were not included since there is no chemical reaction during the welding process. According to this, the exergy of the flow is given as:

$$\dot{E}x_{in} = \overbrace{\dot{E}x_{air}}^{point1} + \overbrace{\dot{E}x_{argon} + \dot{E}x_{CO_2}}^{point4} \tag{16}$$

$$\dot{E}x_{out} = \overbrace{\dot{E}x_{air} + \dot{E}x_{argon} + \dot{E}x_{CO_2}}^{point2} \tag{17}$$

Here, Ex_{air}, Ex_{argon} and Ex_{CO_2} are the exergies of the air and gases used in the welding process. These exergy terms are given as [35]:

$$\dot{E}x_{argon} = \dot{m}_{argon} \bullet C_{p,argon} \bullet \left(T_t - T_0 - T_0 . ln\left(\frac{T_t}{T_{in}}\right) \right) + R_{argon} \bullet T_0 \bullet In\left(\frac{P_t}{P_{atm}}\right) \tag{18}$$

$$\dot{E}x_{CO_2} = \dot{m}_{CO_2} \bullet C_{p,CO_2} \bullet \left(T_t - T_0 - T_0 . \left(\frac{T_t}{T_{in}}\right) \right) + R_{argon} \bullet T_0 \bullet In\left(\frac{P_t}{P_{atm}}\right) \tag{19}$$

$$\begin{aligned} \dot{E}x_{air} = {} & \dot{m}_{air} \bullet \left(C_{p,air} + \omega_{air} . C_{vair}\right) \bullet T_0 \\ & \bullet \left[\left(\frac{T_{in}}{T_0}\right) - 1 - In\left(\frac{T_{in}}{T_0}\right) \right] + (1 + 1.6078 \bullet \omega_{air}) \bullet R_a \\ & \bullet T_0 . In\left(\frac{P_{in}}{P_0}\right) + R_a \\ & \bullet T_0 \bullet (1 + 1.6078 \bullet In\left(\frac{(1 + 1.6078) \bullet \omega_0}{(1 + 1.6078) \bullet \omega_{air}}\right) + (1 + 1.6078) \bullet \omega_{air} \\ & \bullet In\left(\frac{\omega_{air}}{\omega_0}\right) \end{aligned} \tag{20}$$

with

$$\omega_{air} = \frac{0.622 \varphi P_{sat,T}}{P_2 - \varphi P_{sat,T}} \tag{19}$$

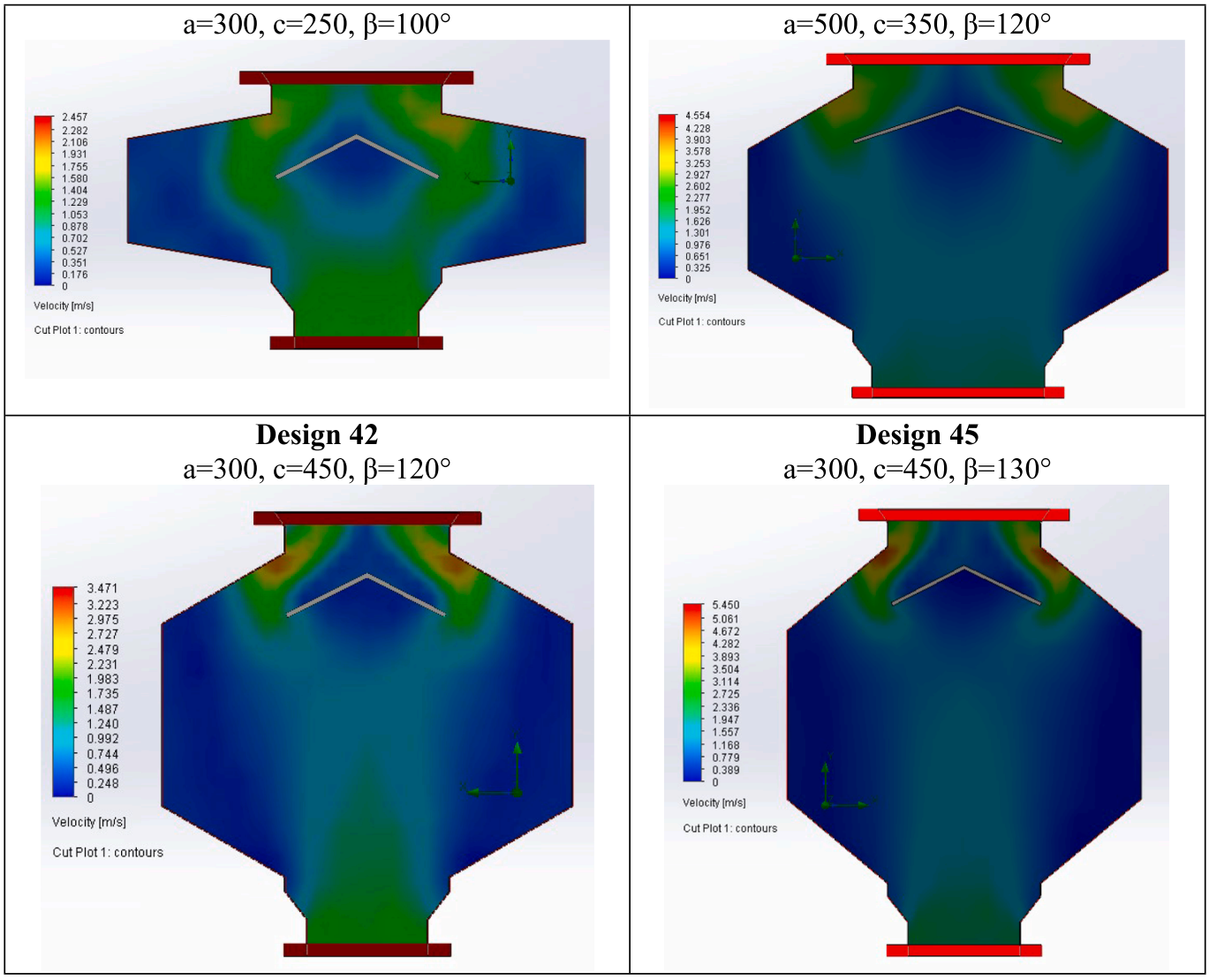

Fig. 11. (*continued*).

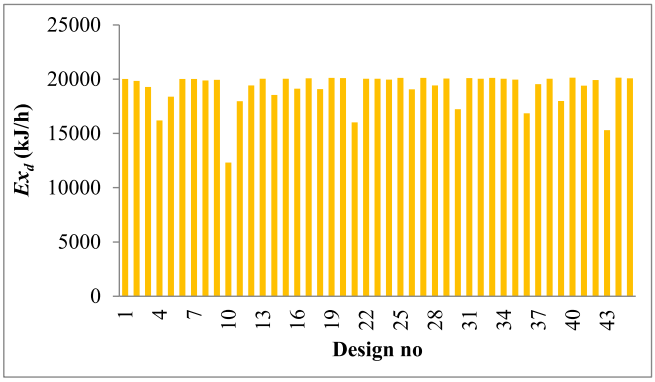

Fig. 12. The effect of β angle and c dimension on Ex_d under summer conditions.

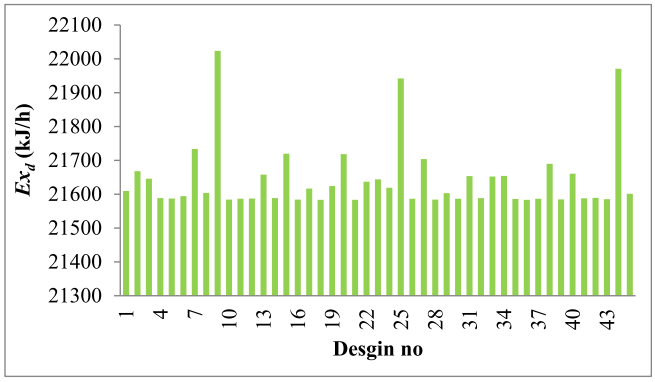

Fig. 13. The effect of β angle and c dimension on Ex_d under winter conditions.

where R_{argon} is is the gas constant of argon (0.208 kJ/kgK), and R_{CO_2} is the gas constant of CO_2 (0.188 kJ/kgK). $E_{x,ec}, E_{x,wo}$ are the exergy of electric consumption of the building and the exergy of workers, respectively [28,35]:

$$\dot{E}x_{ec} = \dot{W}_{ec} \tag{22}$$

$$\dot{E}x_{wo} = n_{wo} \bullet 280 \tag{23}$$

Here, n_{wo} is the number of workers in the building and taken as 15

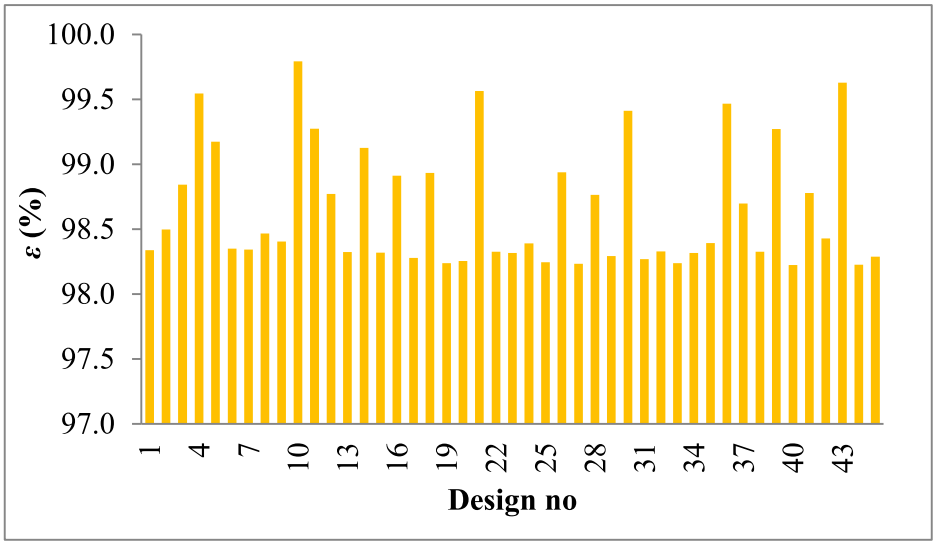

Fig. 14. The effect of β angle and c dimension on ε under summer conditions.

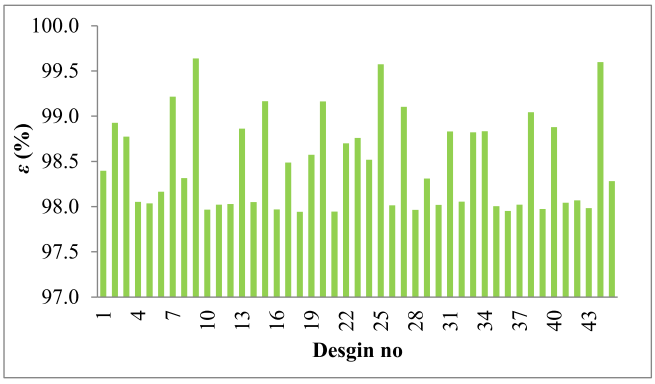

Fig. 15. The effect of β angle and c dimension on ε under winter conditions.

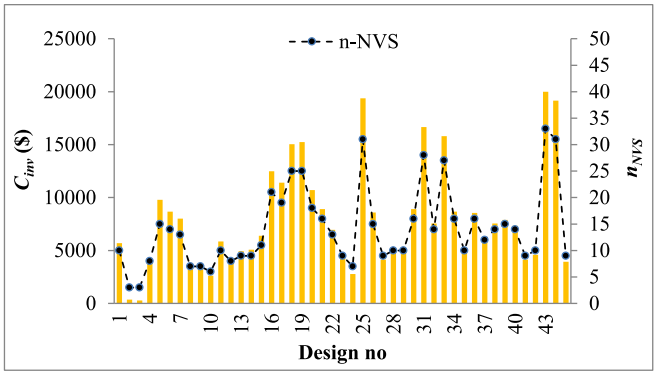

Fig. 16. The variation of initial investment cost (C_{inv}) and the required NVS number (n_{NVS}).

people [28]. The exergy efficiency of the system and sustainability index (SI) are given as [20]:

$$\varepsilon = 1 - \frac{\dot{E}x_d}{\dot{E}x_{in}} \tag{24}$$

$$SI = \frac{1}{1-\varepsilon} \tag{25}$$

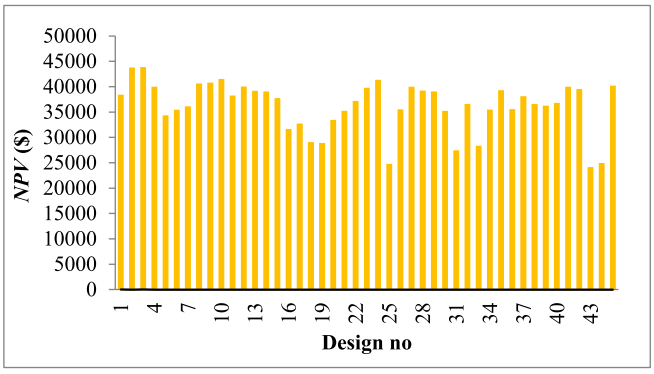

Fig. 17. NPV values of designs.

2.6. Economic and environmental evaluation

For the economic evaluation, net present values (NPV) analysis was handled since it considers the time value of the money for the lifecycle (20 years) of the system. NPV is defined as [36,37]:

$$NPV = \sum_{t=0}^{n} \frac{C_{cf}}{(1+r)^t} - C_{inv} \tag{26}$$

where C_{cf} is the cash flow, C_{inv} is the investment cost, r is the inflation rate of 14.75 % [38] and is the related year of the system's lifetime. The investment cost includes the cost of pipe (C_p), galvanized sheet (C_{st}), welding material (C_W), and labor cost (C_L). The initial investment cost, considering the salvage cost (C_s) of the system and the required fan cost for the conventional ventilation case at the end of the lifetime, is given as follows:

$$C_i = C_p + C_{st} + C_L + C_W - C_s - C_{fan} \tag{27}$$

C_s is the 10 % sum of the other investment terms [36]. C_{fan} is fan cost (237 $/piece) when the conventional forced ventilation by fans is considered [39]. The annual cash flow was obtained considering a mechanical ventilator system instead of the NVS. For an annual working time of 8760 h, the cash flow is defined as [5,28]:

$$C_{cf} = \dot{W}_e \bullet f_e \bullet 8760 \tag{28}$$

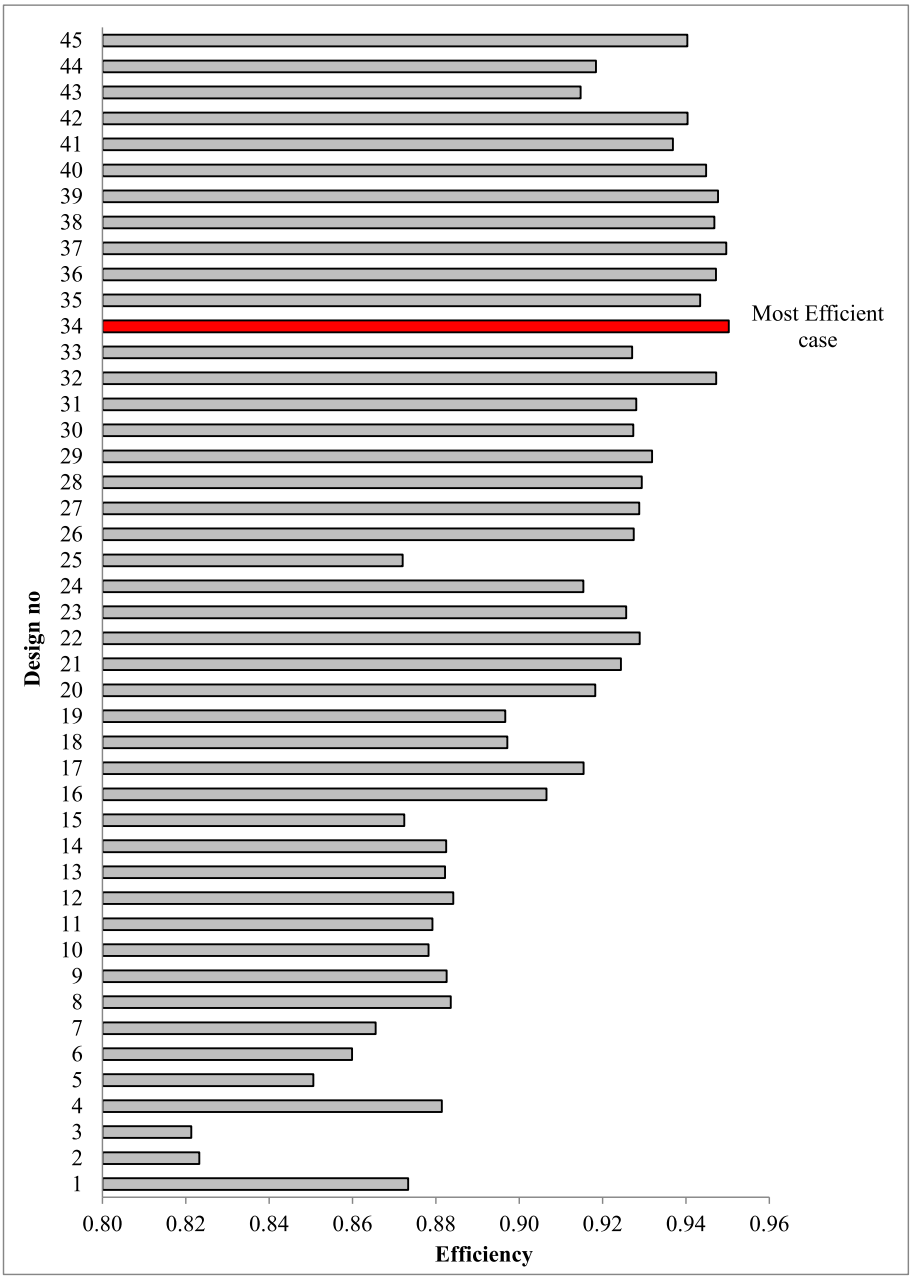

Fig. 18. EATWOS results of the proposed designs.

Here, W_e is the required power of the fan, and f_e is the unit electricity price (0.194 $/h). In the NPV analysis, the benefits were determined by considering the mechanical ventilation requirements for the exact parameters of NVS. In this case, it was assumed that the required ventilation was observed by the fans with an electrical motor of 1.1 kW (W_e) and a ventilation rate of 10,500 m^3/h [30]. The system operates 2503 h annually considering 8 working hours per day, 6 days per week. The saved electricity via NVS also means a saving in natural gas (NG) consumption since an NG-sourced power plant supplies the company's electricity requirement. The annual savings of NG (in mole) is given by [5]:

$$n_{NG} = \frac{W_e \bullet 2503}{HV \bullet \eta_{te}} \tag{29}$$

Here, HV is the heating value (38330 kJ/h), and η_{te} is the efficiency of the power plant (38 %). The saved NG would also decrease the emissions sourced by the combustion of NG in the power plant. The emissions that occurred by NG combustion are given in Table 4 [40,41].

2.7. Optimal design

Multi-criteria decision-making (MCDM) analysis is a useful tool for the optimization of many systems with multi-criteria. Efficiency Analysis Technique with Output Satisficing (EATWOS) is one of the most used MCDM techniques for energy systems [36,42,43]. In terms of the outputs (y) and inputs (x), the efficiency score of EATWOS is given as [44,45]:

Table 6
The results of economic evaluation for Design 34 (in US$).

	Years Present	5	10	15	20
Investment (C_{inv})					
Piping (C_p)	−4,026.07				
Sheet Metal (C_{st})	−3,696.20				
Welding (C_w)	−1,696.45				
Labour (C_L)	−3,631.06				
Total	−13,049.79				
Cash flow					
Benefit from electricity saving (C_{cf})		6,954.18	6,954.18	6,954.18	6,954.18
Fan saving (C_{fan})	3,081.86	–	–	–	–
Salvage (C_s)	1,304.98	–	–	–	–
Total Cash Flow	−8,662.95	6,954.18	6,954.18	6,954.18	6,954.18
The Discount Rate (14.75 %)	1.00	0.50	0.16	0.12	0.06
Present value	−8,662.95	3,495.28	1,756.79	882.99	443.80
NPV	35,475.20				

US$=15.44£.

Table 7
The results of environmental evaluation.

Saving	Unit	Yearly basis	Lifecycle basis
Natural Gas (NG)	m^3	8,846.107	176,922.138
Electricity	GWh	0.036	0.716
CO_2	ton	16.585	331.709
CO	ton	0.005	0.099
NO_x	ton	0.418	8.365

$$E_i = \frac{\sum_{j=1}^{J} v_j \left(1 + \frac{y_{i,j}}{\sqrt{\sum_{j}^{J} y_{i,j}^2}} - \max_i \left\{ \frac{y_j}{\sqrt{\sum_{j}^{J} x_j^2}} \right\} \right)}{\sum_{k=1}^{K} w_k \cdot \left(1 + \frac{x_{i,k}}{\sqrt{\sum_{i}^{K} x_{i,k}^2}} - \min_i \left\{ \frac{x_k}{\sqrt{\sum_{i}^{K} x_k^2}} \right\} \right)} \quad (30)$$

where v and w are the weights input and output parameters, respectively. The pure numeric values of the inputs, such as temperature, and flow rate, which are the direct design parameters, are frequently used in EATWOS to make a decision on the optimal design of the energy systems. However, non-direct parameters about the system related to building structure sometimes should be considered for better operational conditions. Therefore, the input values were selected as the number of the required NVS (n_{NVS}) and the bottom surface area (A_{bottom}) to obtain a homogenous ventilation with a smaller location on the building. Since EATWOS aims for maximum output with the minimum input, the required number is included in the analysis as the reverse form ($1/n_{NVS}$). The output was selected as *SI*, ε, and *NPV*.

3. Results and discussion

Forty-five different natural ventilation systems, designed to achieve the optimum ventilation design regarding techno-economic aspects, were analyzed under the specified boundary conditions as indicated in Table 5, following the validation of CFD analysis and experimental studies.

90 CFD analyses were conducted using FloEFD for the 45 designs under the specified boundary conditions in Table 4, including both summer and winter. Based on the analysis results, the $Q_{T,CFD}$ values were calculated for all 45 designs, considering both summer and winter conditions. The physical design used in the experimental study is represented as the 23rd design among these 45 different designs [28].

The effect of dimensional parameter changes on the ventilation flow rate was determined through FloEFD analysis. The variations in exergy destruction and exergy efficiencies were also calculated for different ventilation designs. Fig. 5 shows the effect of β angle and c dimension on the flow rate for $a = 1200$ mm under summer conditions. Fig. 6 shows the effect of β angle and c dimension on the flow rate for $a = 1200$ mm under winter conditions. Similarly, Figs. 7 and 8 demonstrate the effect of β angle and c dimension for $a = 500$ mm, whereas Figs. 9 and 10 demonstrate the effect of β angle and c dimension for $a = 300$ mm.

According to Figs. 5 to 10, the highest ventilation rate was observed as 32.54 m^3/s for Design 10 (a = 1200, c = 350, β = 130), while the lowest one was observed as 1.17 m^3/s for Design 44 (a = 300, c = 450, β = 120) under the summer conditions. The highest ventilation rate was observed as 30.64 m^3/s for Design 9 (a = 1200, c = 350, β = 120), while the lowest one was observed as 1.13 m^3/s for Design 43 (a = 300, c = 450, β = 110) under the winter conditions. The ventilation rates are higher than the design models with a = 500 mm and a = 300 mm. The base reason for this is the increase in the cross-sectional area through which the air passes, resulting in an increase in ventilation rate due to the thermal buoyancy effect and the pressure difference caused by the wind. When considering Figs. 9 and 10, a moderate level of ventilation performance is observed. This is because of the decrease in the cross-sectional area through which the air passes when a = 500 mm. The effects of the variations in other parameters, such as c and β, can also be observed through the local changes, as seen in Figs. 7 to 9. When considering Figs. 9 and 10, the lowest ventilation performances are observed. It can be concluded that the variation in the dimension generally has a linear effect on the changes in $Q_{T,CFD}$ values, indicating that as the dimensions increase, the $Q_{T,CFD}$ values also increase. However, when considering the variations in the β angle and c dimension locally, it was observed that there is not always a proportional increase in the $Q_{T,CFD}$ values. In the cases with β = 120° and height c = 350, reasonable results were obtained because the area between the apparatus close to the exit and the inclined part of the NVS relieved the flow exit. In some cases, there were decreases in the $Q_{T,CFD}$ values.

Velocity contours for different designs are given in Fig. 11. When these graphs are examined, as the width decreases, the flow velocity drawn from the environment increases, and it is directed more towards the outlet. When a = 300 mm, the cross-sectional area is significantly reduced, which also increases thermal buoyancy and wind-driven ventilation capabilities. The base reason for this is the increase in the cross-sectional area through which the air passes, resulting in an increase in ventilation rate due to the thermal buoyancy effect and the pressure difference caused by the wind. As the height increases, the fluid velocity and, therefore, the fluid flow rate increases. In addition, as the angle increases, the flow direction becomes easier, and the flow becomes smoother.

The changes in the exergy destruction (Ex_d) and exergy efficiency (ε) values for the 45 different designs were determined depending on the dimensional parameters. Fig. 12 illustrates the effect of the variation in the β angle and c dimension on the changes in Ex_d under summer conditions, while Fig. 13 demonstrates the impact of the variation in the β angle and c dimension on the changes in Ex_d under winter conditions.

When evaluating Fig. 12 and Fig. 13, it can be observed that Design 9 (a = 1200, c = 350, β = 120) has the highest exergy destruction value with Ex_d = 22023.66 kJ/h under winter conditions, while Design 40 (a = 300, c = 350, β = 130) has the highest one withEx_d = 20136.54 kJ/h under summer conditions. On the other hand, Design 10 has the lowest exergy destruction value withEx_d = 12310.83 kJ/h under summer conditions, whereas Design 18 has the lowest one withEx_d = 21583.10 kJ/h under winter conditions. The variation in exergy destruction values among designed models is due to the difference in the amount of discharged air, which depends on the required NVS. Fig. 14 illustrates the

effect of the variation in the β angle and c dimension on the changes in exergy efficiency (ε) under summer conditions, while Fig. 15 demonstrates the impact of the variation in the β angle and c dimension on the changes in ε under winter conditions.

When evaluating Fig. 14 and Fig. 15, it can be observed that Design 10 (a = 1200, c = 350, β = 130) has the highest exergy efficiency value with ε = 99.07 % under summer conditions, and Design 9 (a = 1200, c = 350, β = 120) has the highest exergy efficiency value with ε = 98.83 % under winter conditions. On the other hand, Design 44 (a = 300, c = 450, β = 120) has the lowest exergy efficiency value with ε = 98.23 % under summer conditions, and Design 18 (a = 500, c = 250, β = 110) has the lowest exergy efficiency value with ε = 97.94 % under winter conditions. The variation in exergy efficiency values among designed models is caused by the difference in the amount of discharged air, which depends on the design. As a result, NVS models designed to provide higher ventilation discharge are associated with higher Ex_{in} values, leading to higher exergy efficiency values. In the studied building, which is the subject of the experimental work, it is desired to ventilate the total building volume (130,165.0 m^3) once per hour [15]. According to this, the required number of NVS (n_{NVS}) and regarding investment cost (C_{inv}) are given in Fig. 16.

For the existing design (Design 23), the required number of units n_{NVS} was determined as 9. The minimal number was determined as 3 for the Design 2 and 3, while the maximum was determined as 33 for the Design 43. The NPV values were calculated for the 45 different designs, considering a 20-year lifetime, and graphically represented in Fig. 17.

For the existing design, the NPV value was calculated as 39,785.82 $ at the end of the 20-year lifetime of the experimental study. In the NPV calculation based on CFD analysis, as shown in Fig. 18, the highest NPV value of 43,849.15 $ was achieved for Design 3, whereas the lowest NPV was 24,148.30 $ for Design 43. According to economic evaluation, the best design was determined as Design 3 with the highest NPV value. However, the required number of NVS was observed as Design 3 in this design. Hence, local ventilation is available in the building, which does not allow homogenous ventilation.

According to the exergetic evaluation, the best design was determined as Design 10 with a required NVS number of 6 for the summer conditions, whereas the best design was determined as Design 10 with a required NVS number of 7 for the winter conditions. These numbers also cannot be enough for a homogenous ventilation. Undoubtedly, more NVS would be better for this aim. Another parameter was chosen as the covered area of the NVS on the roof. If the area and required area are larger, it would cause more opening area on the roof, which could lead to leakage streams. So, in this study, non-direct parameters of the required number of NVS and the covered area were used in MCDM analysis to determine the best efficient design to observe the highest exergy efficiency, NPV, and SI. The results of the EATWOS analysis are given in Fig. 18.

According to EATWOS results, the most efficient case was determined as Design 34 with a score of 0.9502, whereas the worst one was Design 3 with a score of 0.8213. The required number of NVS for Design 34 was determined as 16, with a covering area of 28.8 m^2. The exergetic efficiency and sustainability index were determined as 98.32 % and 98.83 % 1.24, respectively, in this case. Table 6 presents detailed economic analysis data for a lifetime of 20 years for Design 34.

The annual benefit was calculated as 6,954.18, considering an electricity price (f_e) of 0.194 $/kWh [15]. Finally, the system's NPV value was determined as 35,475.20 $, which means that the NVS is profitable for industrial buildings. The saved emissions were determined based on the saved electricity obtained from the NG-fueled plant, as given in Table 7.

According to Table 6, NG saving of 176,922.14 m^3 during the system lifetime of 20 years is possible. This saving also means avoidance of 331.71 tons of CO_2, 0.10 tons of CO, and 8.37 tons of NO_x.

4. Conclusion

In this study, the natural ventilation of an industrial building was numerically investigated through a newly designed stack-type ventilation system (NVS) first in the literature. CFD analysis was performed to optimize the NVS design by generating different NVS designs. The performance of the designs was evaluated by exergy analyses. The economic evaluation was also performed via net present value (NPV) analysis. The performed designs were optimized through multi-criteria decision-making (MCDM) analysis. In the optimization, non-direct parameters were included into MCDM to obtain a homogenous ventilation of the industrial building. The following conclusions were drawn from the study:

1. The highest NPV value was determined as 43,849.15 $ for Design 3 (a = 1200, c = 450, β = 90), whereas the lowest NPV was determined as 24,148.30 $ for Design 43 (a = 300, c = 350, β = 100). The NPV value of the experimentally investigated one (Design 23; a = 300, c = 350, β = 100) was determined as 39,785.82 $.
2. The designs with the highest exergy efficiency are observed for Design 10 (a = 1200, c = 350, β = 130) with ε = 99.80 % under summer conditions and Design 9 (a = 1200, c = 350, β = 120) with ε = 99.64 % under winter conditions. The designs with the lowest exergy efficiency are observed for Design 40 (a = 300, c = 350, β = 130) with ε = 98.23 % under summer conditions and Design 18 (a = 500, c = 250, β = 110) with ε = 97.94 % under winter conditions.
3. The maximum required number of NVS was determined for Design 3 (a = 1200, c = 350, β = 90) with a covering area of 21.60 m^2. The minimum required number of NVS was determined for Design 43 (a = 300, c = 250, β = 130) with a covering area of 59.40 m^2.
4. The most efficient design was determined for Design 34 (a = 300, c = 250, β = 100) with an NPV value of 35,475.20 $. The minimum required number of NVS was determined for Design 16, with a covering area of 28.80 m^2. The exergy efficiency is observed as 98.32 % for summer and 98.83 % for winter conditions.
5. Design 34 can provide ventilation for the total building volume once per hour in both summer and winter conditions. This implementation enables a saving of 176,922.14 m^3 of natural gas consumption. In this way, it is possible to prevent the emission of 331.71 tons of CO_2 from an environmental perspective.

CRediT authorship contribution statement

Onur Kayapinar: Writing – original draft, Visualization, Methodology, Investigation, Formal analysis, Data curation, Conceptualization. **Aslı E. Arslan:** Writing – original draft, Methodology, Investigation, Formal analysis. **Oguz Arslan:** Writing – review & editing, Validation, Supervision, Methodology, Investigation, Formal analysis, Data curation, Conceptualization. **Mustafa Serdar Genc:** Writing – review & editing, Validation, Software, Methodology, Formal analysis, Data curation.

Declaration of competing interest

The authors declare that they have no known competing financial interests or personal relationships that could have appeared to influence the work reported in this paper.

Data availability

No data was used for the research described in the article.

References

[1] Bhaita A. Natural ventilation principles and practices. Createspace Independent Publishing Platform, 2014.

[2] S.B. Riffat, A study of heat and mass transfer through the doorway in the traditionally built house, ASHRAE Trans. 95 (1989) 573–583.
[3] Z. Gao, J. Cai, P. Wang, M. Liu, L. Li, Smoke exhaust characteristics under stack effect of natural ventilation by shaft in high-altitude tunnel, Therm. Sci. Eng. Progr. 48 (2024) 102397.
[4] A. Boccalatte, M. Fossa, R. Sacile, Modeling, Design and Construction of a Zero-Energy PV Greenhouse for Applications in Mediterranean Climates, Therm. Sci. Eng. Progr. 25 (2021) 101046.
[5] O. Kayapinar, O. Arslan, Time-stepped Exergy Analysis, Environmental and Economic Evaluation of a New Designed Natural Ventilation System, Therm. Sci. Eng. Progr. 44 (2023) 102058.
[6] K. Wang, X. He, L. Sun, X. Hu, Y. Guo, P. Zhang, Numerical study on upstream smoke propagation and induced airflow velocity in a tilted channel under natural ventilation, Therm. Sci. Eng. Progr. 46 (2023) 102228.
[7] M. Vaseghi, M. Fazel, A. Ekhlassi, Numerical investigation of solar radiation effect on passive and active heating and cooling system of a concept museum building, Therm. Sci. Eng. Progr. 19 (2020) 100582.
[8] Z.T. Ai, C.M. Mak, Wind-induced single-sided natural ventilation in buildings near a long street canyon: CFD evaluation of street configuration and envelope design, J. Wind Eng. Ind. Aerodyn. 172 (2018) 96–106.
[9] S.F. Ali, M. Ali, Effects of wall angularity of atrium on buildings natural ventilation and thermal performance and CFD design, J. Energy. Build. 121 (2016) 265–283.
[10] F. Xu, S. Xu, U. Passe, B. Ganapathysubramanian, Computational study of natural ventilation in a sustainable building with complex geometry, J. Suitab. Energy Technol. Assessm. 45 (2021) 101–153.
[11] W. Guo, X. Liu, X. Yuan, Study on Natural Ventilation Design Optimization Based on CFD Simulation for Green Buildings, J. Procedia Eng. 121 (2015) 573–581.
[12] E. Gianpiero, P. Viktor, Computational analysis of wind-driven natural ventilation in buildings, J. Energy Build. 38 (2006) 491–501.
[13] S. Hulsure, R.S. Maurya, Numerical Investigation of Wind Driven Natural Ventilation in a Mega Warehouse Building, Int. J. Fluid Eng. 23 (2019) 1–23.
[14] V.T. Hooff, B. Blocken, Full-scale measurements of indoor environmental conditions and natural ventilation in a large semi-enclosed stadium: Possibilities and limitations for CFD validation, J. Wind Eng. Ind. Aerodyn. 104 (2012) 330–341.
[15] S. Huang, Q.S. Li, S. Xu, Numerical Evolution of Wind Effects on a Tall Steel Building by CFD, J. Constr. Steel Res. 2006 (63) (2006) 612–627.
[16] M. Rafaela, M.C. Jos'e, P. Armando, Natural ventilation of large air masses: Experimental and numerical techniques review, J. Energy Build. 291 (2023) 113–120.
[17] V.H. Twan, B. Bert, L. Aenan, B. Benjamin, A venturi-shaped roof for wind-induced natural ventilation of buildings: Wind tunnel and CFD evaluation of different design configurations, J. Build. Environ. 46 (2011) 1797–1807.
[18] A.E. Arslan, O. Arslan, S.Y. Kandemir, AHP–TOPSIS hybrid decision-making analysis: Simav integrated system case study, J. Therm. Anal. Calorim. 145 (2021) 1191–1202.
[19] Arslan AE. Multi-criteria decision making of Simav integrated geothermal energy system: AHP-EATWOS hybrid analysis. Current Researches in Humanities and Social Sciences. First Edition, Ivpe Cetinje Publications, Montenegro 2020: pp. 83–107.
[20] A.E. Arslan, O. Arslan, M.S. Genc, Hybrid modeling for the multi-criteria decision making of energy systems: An application for geothermal district heating system, Energy 286 (2024) 129590.
[21] X. Yin, M.W. Muhieldeen, R. Razman, J.Y.C. Ee, Multi-objective optimization of window configuration and furniture arrangement for the natural ventilation of office buildings using Taguchi-based grey relational analysis, Energ. Buildings 296 (2023) 113385.
[22] Y. Wen, J. Wei, S.K. Lau, Z. Gu, J. Leng, A two-level optimisation approach for underground natural ventilation based on CFD and building energy simulations, Energ. Buildings 310 (2024) 114102.
[23] P. Liu, H.M. Mathisen, M.J. Alonso, A. Halfvardsson, A multi-objective optimisation framework to design membrane-based energy recovery ventilation for low carbon buildings, Energ. Conver. Manage. 291 (2023) 117298.
[24] A. Buonomano, C. Forzano, G.F. Giuzio, A. Palombo, New ventilation design criteria for energy sustainability and indoor air quality in a post Covid-19 scenario, Renew. Sustain. Energy Rev. 182 (2023) 113378.
[25] S. Zhang, Z. Lin, Z. Ai, C. Huan, Y. Cheng, F. Wang, Multi-criteria performance optimization for operation of stratum ventilation under heating mode, Appl. Energy 239 (2019) 969–980.
[26] N. Bianco, A. Fragnito, M. Iasiello, G.M. Mauro, A CFD multi-objective optimization framework to design a wall-type heat recovery and ventilation unit with phase change material, Appl. Energy 347 (2023) 121368.
[27] Turkish Patent and Trade Mark Office. Patent no: 2019-08313.
[28] Kayapinar O. Using of Natural Ventilation System for Disposal of Breathable Gases in Production Lines and Improving Indoor Air Quality, Ph.D. Dissertation, Institute of Applied Sciences, Bilecik Seyh Edebali University, 2023.
[29] Trebunskikh TV, Ivanov AV, Dumnov GE. FloEFD simulation of micro-turbine engine. In Proceedings of Applied Aerodynamics Conference on Modelling & Simulation in the Aerodynamic Design Process: Vol. 1, New York: Curran Associates, Inc., pp. 51-64, 2012.
[30] Genc MS., Ozden KS. Flow Physics Analysis of a Vertical Axis Wind Turbine Using FloEFD. In Proceedings of 7th Iran Wind Energy Conference (IWEC2021), pp. 1-4, May 17th, 2021.
[31] Hetyeia C, Molnár I, Szlivkab F. Spatial Arrangement of a Counter-Rotating Dual Rotor Wind Turbine. EasyChair Preprint, No. 10016, 2023.
[32] I. Karasu, M. Ozden, M.S. Genc, Performance assessment of transition models for three-dimensional flow over NACA4412 wings at low Reynolds numbers, J. Fluids Eng. 140 (2018) 121102.
[33] H. Arat, O. Arslan, U. Ercetin, A. Akbulut, A comprehensive numerical investigation of unsteady-state two-phase flow in gravity assisted heat pipe enclosure, Therm. Sci. Eng. Progr. 25 (2021) 100993.
[34] NIST Chemisty Web-Book: NIST Standart Reference Database, No: 69, 2023. Available from: http://webbook.Nist.gov/chemistry.
[35] A. Hepbasli, A Key Review on Exergetic Analysis and Assessment of Renewable Energy Resources for a Sustainable Future, Renew. Sustain. Energy Rev. 12 (2008) 593–661.
[36] O. Arslan, A.A. Ergenekon, Performance evaluation and multi-criteria decision analysis of thermal energy storage integrated geothermal district heating system, Process Saf. Environ. Prot. 167 (2022) 21–33.
[37] O. Arslan, D. Kilic, Concurrent optimization and 4E analysis of organic Rankine cycle power plant driven by parabolic trough collector for low-solar radiation zone, Sustain. Energy Technol. Assess. 46 (2021) 101230.
[38] Central Bank of Republic of Turkey, Exchange and inflation rates, Available from: https://tcmb.gov.tr. Last access: May 27th, 2022.
[39] GETA, Fans for mechanical ventilation. Available from: https://www.makinabizde.com/GETA-GVAK-6306-11-kw-1000-DD-380-V-Trifaze-Kanal-Tipi-Aksiyal-Fan, PR-6889.html. Last Acces: November 12th, 2023.
[40] O. Arslan, M.A. Ozgur, H.D. Yildizay, R. Kose, Fuel Effects on Optimum Insulation Thickness: An Exergetic Approach, Energy Sour. Part A 32 (2009) 128–147.
[41] O. Arslan, M. Ucar, Assessment of improvement potential of condensed combi boiler via advanced exergy analysis, Therm. Sci. Eng. Progr. 23 (2021) 100853.
[42] O. Arslan, A.E. Arslan, T.E. Boukelia, Modelling and optimization of domestic thermal energy storage based heat pump system for geothermal district heating, Energ. Buildings 282 (2023) 112792.
[43] O. Arslan, A.E. Arslan, I. Kurtbas, Exergoeconomic and exergoenvironmental based multi-criteria optimization of a new geothermal district heating system integrated with thermal energy storage driven heat pump, J. Build. Eng. 73 (2023) 106733.
[44] M.L. Peters, S. Zelewski, "Efficiency analysis under consideration of satisficing levels for output quantities," in *Proc. of the 17th Annual Conference of the Production and Operations Management Society*, Boston, USA, 2006, pp. 2-18.
[45] O. Arslan, A.E. Arslan, Multi-criteria optimization of a new geothermal driven integrated power and hydrogen production system via a new Index: Economic sustainability (EcoSI), Fuel 58 (2024) 130160.